THEORY OF MICROWAVE INSTABILITY AND COHERENT SYNCHROTRON RADIATION IN ELECTRON STORAGE RINGS*

Yunhai Cai†, SLAC National Accelerator Laboratory, Menlo Park, CA 94025, USA

Abstract

Bursting of coherent synchrotron radiation has been observed and in fact used to generate THz radiation in many electron storage rings. In order to understand and control the bursting, we return to the study of the microwave instability. In this paper, we will report on the theoretical understanding, including recent developments, of the microwave instability in electron storage rings. The historical progress of the theories will be surveyed, starting from the dispersion relation of coasting beams, to the work of Sacherer on a bunched beam, and ending with the Oide and Yokoya method of discretization. This theoretical survey will be supplemented with key experimental results over the years. Finally, we will describe the recent theoretical development of utilizing the Laguerre polynomials in the presence of potential-well distortion. This self-consistent method will be applied to study the microwave instability driven the impedances due to the coherent synchrotron radiation.

INTRODUCTION

Over the past quarter century, there has been steady progress toward smaller transverse emittances in electron storage rings used for synchrotron light sources, from tens of nm decades ago to the nm range recently. In contrast, there is not much progress made in the longitudinal plane. For an electron bunch in a typical ring, its relative energy spread σ_δ remains about 10^{-3} and its length σ_z is still in between 5 mm to 10 mm. Now the longitudinal emittance $(\sigma_\delta\sigma_z)$ becomes a factor of thousand larger than those in the transverse dimensions. In this paper, we will address questions of: How short a bunch can be? What is the fundamental limit? If there is a limit, is there any mitigation method? Since the synchrotron radiation is so fundamental in electron storage rings, let us start with the coherent synchrotron radiation (CSR).

COASTING BEAM THEORY

If one studies a perturbation $\Psi_1 = \Psi(\delta)e^{-i\Omega s/c + ikz}$ for an electron beam with an energy of $E_0 = \gamma mc^2$, a current I, and a Gaussian distribution with a relative energy spread σ_δ, one can derive (for example see[1])

$$1 = i\frac{cI}{\alpha\gamma\sigma_\delta^2 I_A}\left(\frac{\hat{Z}(k)}{k}\right)\int_{-\infty}^{\infty}\frac{dF_0/dp}{p-a}dp, \quad (1)$$

based on the linearized Vlasov equation of coasting beam. Here $I_A = mc^3/e = 17045$ A is the Alfven current, α the momentum compaction factor, $\hat{Z}(k)$ the impedance per unit length, and $F_0 = e^{-p^2/2}/\sqrt{2\pi}$. In general, $a = \Omega/\alpha ck\sigma_\delta$, is a complex number and is to be solved for a given value of k. One can see that there is a pole on the real axis in the integral in Eq. (1). The correct treatment of the pole leads to the Landau damping. Actually, one can first evaluate the integral in the upper half plane and then analytically continue it into the lower half plane. The result of the integral is given by

$$G(a) = -1 + \sqrt{\frac{\pi}{2}}ae^{-a^2/2}(\text{erfi}(\frac{a}{\sqrt{2}}) - i). \quad (2)$$

It is easy to see from the perturbation that the beam is unstable if $\text{Im}[\Omega] > 0$.

CSR Impedance in Free Space

For electrons, orbiting on a circle with radius ρ inside bending magnets, the longitudinal wakefield due to the steady CSR in free space was given by Murphy, Krinsky, and Gluckstern[2]

$$W_{csr}(z) = -\frac{4\pi\rho^{1/3}}{(3z)^{4/3}}, \quad (3)$$

for $z > 0$ and the wake vanishes when $z < 0$. Unlike a conventional wake, the CSR force is acting on the electron ahead. Its corresponding impedance was actually found by Faltens and Laslett[3]

$$Z_{csr}(k) = (\frac{2\pi}{c})\frac{\Gamma(2/3)(\sqrt{3}+i)}{3^{1/3}}(\rho k)^{1/3}, \quad (4)$$

where Γ is the Gamma function.

Microbunching

Using $\hat{Z}_{csr}(k) = Z_{crs}(k)/2\pi\rho$, Stupakov and Heifets[1] analyzed the dispersion relation of Eq. (1) and showed that the beam becomes unstable if

$$k\rho < 2.0\Lambda^{3/2}, \quad (5)$$

where $\Lambda = I/\alpha\gamma\sigma_\delta^2 I_A$. In this model, given a current, there is always an unstable mode when its wave number k is low enough.

This stability condition was confirmed[4] experimentally at the Advanced Light Source, where the evidence of microbunching in the bolometer signal was found when the bunch current

$$I_b > \frac{\pi^{1/6}\alpha\gamma\sigma_\delta^2 I_A\sigma_z}{\sqrt{2}\rho^{1/3}\lambda^{2/3}}, \quad (6)$$

05 Beam Dynamics and Electromagnetic Fields

D03 High Intensity in Circular Machines

for the wavelengths at $\lambda = 2$ mm and $\lambda = 3.2$ mm at various beam energies. This expression can be derived from Eq. (5) provided,

$$I = \sqrt{2\pi}\rho I_b/\sigma_z, \tag{7}$$

which is a result of identifying the peak current of the bunched beam with I.

CSR Impedance with Shielding

The calculation of the exact impedance with the shielding from two parallel metal plates, separated by a distance h, was carried out by Warnock[5] in terms of the Bessel functions. Utilizing the uniform asymptotic expansion[6] of the Bessel functions, one can approximate the impedance with the Airy functions Ai and Bi,

$$\left(\frac{\rho}{h}\right)\left(\frac{Z(n)}{n}\right)_{csr\_p} = \frac{16\pi^3 2^{1/3}}{c}[n(\frac{h}{\rho})^{3/2}]^{-4/3}$$
$$\times \sum_{p>=1,3,...} [Ai'(u)Ci'(u) + uAi(u)Ci(u)], \tag{8}$$

where $n = k\rho$, $Ci = Ai - iBi$, and u is defined as

$$u = \frac{\pi^2 p^2}{2^{2/3}}[n(\frac{h}{\rho})^{3/2}]^{-4/3}. \tag{9}$$

Note that the dependency of n on the left side of the equation is all through $n(h/\rho)^{3/2}$. This kind of scaling law was proposed as an approximated property by Murphy, Krinsky, and Gluckstern[2]. In fact, one can show that Eq. (8), gives the impedance that corresponds to their wakefield, which was used in our recent simulations[7].
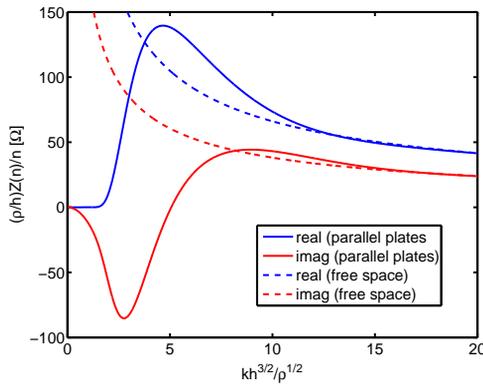

Figure 1: Scaled Z(n)/n for the CSR impedances in parallel plates and in free space.

Moreover, the same scaling property holds for the CSR impedance in free space as well; formally Eq. (4) can be rewritten as,

$$\left(\frac{\rho}{h}\right)\left(\frac{Z(n)}{n}\right)_{csr} = \left(\frac{2\pi}{c}\right)\frac{\Gamma(2/3)(\sqrt{3}+i)}{3^{1/3}}$$
$$\times[n(\frac{h}{\rho})^{3/2}]^{-2/3}. \tag{10}$$

05 Beam Dynamics and Electromagnetic Fields

D03 High Intensity in Circular Machines

The scaled impedances written in Eqs. (8) and (10) are plotted in Fig 1. As one can see in the figure, for the parallel plate model, its real part becomes zero near $kh^{3/2}/\rho^{1/2} = 2$ at the low end of frequency. Clearly, there is a strong shielding effect at the long wavelength by the metal plates. At the end of short wavelength, its impedance is asymptotically approaching the impedance in free space as it should be.

Stability Analysis with Shielding

Using the impedance defined in Eq. (8), we analyzed the dispersion relation of Eq. (1) for various values of a scaled current, $S = Ih/\alpha\gamma\sigma_\delta^2 I_A\rho$, as shown in Fig. 2. The dispersion curves clearly show the shielding effect at the low end of $kh^{3/2}/\rho^{1/2}$. As one can see, the beam is stable for all values of the wave number when $S < 6/\pi$. The threshold of the instability occurs at the current of $S^{th} = 6/\pi$ with

$$k^{th} = 5.7\rho^{1/2}/h^{3/2}. \tag{11}$$

Above the threshold, the lowest unstable wave number is also proportional to $\rho^{1/2}/h^{3/2}$; However, its coefficient varies as a function of the current and is not a fixed value as suggested in many previous publications.
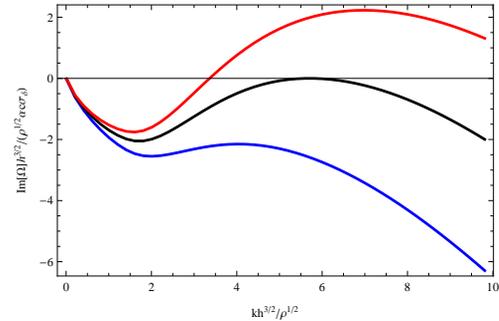

Figure 2: Scaled imaginary part of the dispersion curves with three values of the scaled current $S = 1, 6/\pi, 3$ in the color of blue, black, and red respectively.

To compare the theory with the observations, we need to use Eq. (7) to rewrite the instability condition, $S > 6/\pi$, in terms of the bunch current,

$$I_b > \frac{3\sqrt{2}\alpha\gamma\sigma_\delta^2 I_A\sigma_z}{\pi^{3/2}h}. \tag{12}$$

Note that the threshold does not depend on ρ.

Table 1: Measurements in the NSLS VUV Ring

Parameter	Measurement	Theory
Threshold wavelength, λ^{th}	7.0 mm	6.9 mm
Threshold current, I_b^{th}	100 mA	134 mA

A comparison of the theory, using Eqs. (11) and (12), with the observation[8] in the VUV ring of the National

Synchrotron Light Sources at BNL is presented in Table 1. As one can see, the agreement in the wavelength of the unstable mode is excellent. The calculated threshold is 30% higher than the measured value.

BUNCHED BEAM THEORY

In a storage ring, electrons inside a bunched beam execute synchrotron oscillation at frequency $f_s = \nu_s f_{rev}$, where f_{rev} is the revolution frequency. The synchrotron tune ν_s is given by

$$\nu_s = \sqrt{\frac{\alpha f_{rf}}{2\pi f_{rev}}(\frac{eV_{rf}}{E_0})\cos\phi_s},\qquad(13)$$

where f_{rf} is the RF frequency. The RF voltage V_{rf} is necessary to compensate the energy loss U_0 due to the synchrotron radiation in every turn of the circulation, namely $U_0 = eV_{rf}\sin\phi_s$. The equilibrium bunch distribution is a Gaussian. The bunch length is given by[9]

$$\sigma_z = \alpha c\sigma_\delta/\omega_s,\qquad(14)$$
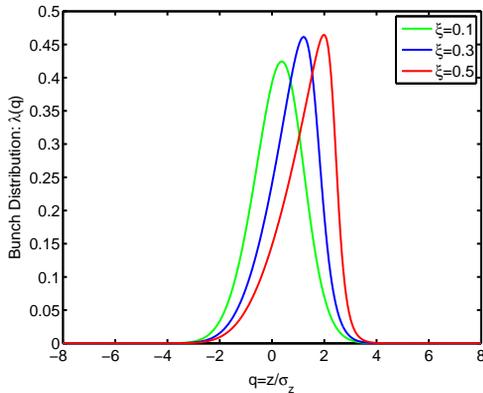
where $\omega_s = 2\pi f_s$.

Figure 3: Haissinski distributions at various scaled currents, $\xi = 0.1, 0.3, 0.5$, for the CSR in free space. The head of the bunch is to the right.

When there are longitudinal wakefields in the storage ring, the equilibrium becomes a Haissinski distribution[10] at a sufficiently low bunch current. For the wakefield driven by the CSR in free space in Eq. (3), the Haissinski distributions are shown in Fig. 3. To study the stability at a higher current, one can make a small perturbation near the Haissinski distribution and then analyze the linearized Vlasov equation for the perturbation. This leads to an set of integral equations[11, 12].

Sacherer Integral Equation

For all azimuthal mode number $l = -\infty,...\infty$, we have the integral equation

$$(\frac{\Omega}{\omega_s} - l\frac{\omega(K)}{\omega_s})P_l(K) =$$

$$\sum_{m=-\infty}^{\infty}\int_0^{\infty}dK'G_{l,m}(K,K')P_m(K').\quad(15)$$

Its kernel is given by

$$G_{l,m}(K,K') = \frac{-\sqrt{2}lI_nce^{-(K+V_{min})}}{\sqrt{\pi}\kappa\sigma_z}$$
$$\times\mathrm{Im}[\int_0^{\infty}d\nu\frac{Z(\nu/\sigma_z)}{\nu}h_l(\nu,K)h_m^*(\nu,K')],\,(16)$$

where

$$h_l(\nu,K) = \int_0^{2\pi}\frac{d\phi}{2\pi}e^{-il\phi+i\nu q(\phi,K)}.\qquad(17)$$

Here we have the normalized current

$$I_n = \frac{r_eN_b}{2\pi\nu_s\gamma\sigma_\delta},\qquad(18)$$

where $r_e = e^2/mc^2$ is the classic radius of electron and N_b the bunch population. It can be rewritten in terms of the bunch current I_b,

$$I_n = \frac{\sigma_zI_b}{\alpha\gamma\sigma_\delta^2I_A},\qquad(19)$$

using Eq. (14). κ, V_{min}, $\omega(K)$, and $q(\phi,K)$ can be determined by the underling Haissinski distribution. Since the Haissinski solution is a function of the current, they depend on I_n as well.

Given a current I_n, one needs to solve $P_l(K)$ for all l along with Ω. When $\mathrm{Im}[\Omega] > 0$, the beam is unstable. One method to solve the integral equations is to discretize[11] the variable K. Here we will present an alternative.

Polynomial Expansion

Using the generalized Laguerre polynomials $L_\alpha^{|l|}(K)$, we decompose

$$P_l(K) = e^{-K}\sum_{\alpha=0}^{\infty}a_l^\alpha f_\alpha^{(l)}(K),\qquad(20)$$

where

$$f_\alpha^{(l)}(K) = \sqrt{\frac{\alpha!}{(|l|+\alpha)!}}K^{|l|/2}L_\alpha^{|l|}(K).\qquad(21)$$

Applying the orthogonal and normal condition of the Laguerre polynomials, we reduce the Sacherer integral equations to a set of linear equations,

$$\frac{\Omega}{\omega_s}a_\alpha^l = \sum_{m=-\infty}^{\infty}\sum_{\beta=0}^{\infty}M_{l,m}^{\alpha,\beta}a_\beta^m,\qquad(22)$$

for $l = -\infty,...\infty$ and $\alpha = 0,...\infty$.

Clearly, it becomes an eigen value problem. Ω/ω_s is the eigen value. In fact, M is a real matrix. When the current is small, all eigen values are real and therefore the beam is

05 Beam Dynamics and Electromagnetic Fields

D03 High Intensity in Circular Machines

stable. It becomes unstable, when the first pair of complex value emerges as the current increases.

The matrix elements are given by

$$M_{lm}^{\alpha\beta} = l(\delta_{lm}O_{(l)}^{\alpha\beta} - C_{lm}^{\alpha\beta}) \tag{23}$$

and

$$O_{(l)}^{\alpha\beta} = \int_0^\infty dK \frac{\omega(K)}{\omega_s} e^{-K} f_\alpha^{(l)}(K) f_\beta^{(l)}(K), \tag{24}$$

$$C_{lm}^{\alpha\beta} = \frac{\sqrt{2} I_n c e^{-V_{min}}}{\sqrt{\pi}\kappa\sigma_z}$$
$$\times \mathrm{Im}[\int_0^\infty d\nu \frac{Z(\nu/\sigma_z)}{\nu} g_l^\alpha(\nu) g_m^{\beta\,*}(\nu)], \tag{25}$$

where

$$g_l^\alpha(\nu) = \int_0^\infty dK e^{-K} f_\alpha^{(l)}(K) h_l(\nu, K). \tag{26}$$

Now, the problem of analyzing the instability of bunched beam is reduced to first evaluating the integrals in Eqs. (17), (26), (24), and (25), and then finding the eigen values and eigen vectors of the matrix M.

Instability Driven by the CSR in Free Space

For the impedance given by Eq. (4), a complete analysis of the stability of the Haissinski distribution as a function of the current was carried out[12]. As shown in Fig 4, the threshold of the instability is at $\xi^{th} = 0.482$.
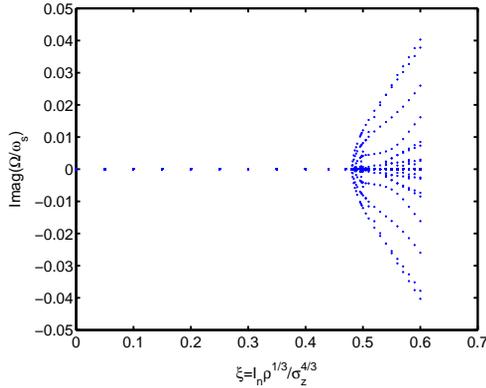

Figure 4: Imaginary part of the eigen values for Ω/ω_s as a function of the scaled current, $\xi = I_n \rho^{1/3}/\sigma_z^{4/3}$, for the impedance driven by the CSR in free space.

Threshold of the CSR Instability with Shielding

Similar analysis is carried out using the impedance defined in Eq (8). Because of the additional parameter h and the scaling property in the impedance formula, the threshold becomes a function of the shielding parameter, $\chi = \sigma_z \rho^{1/2}/h^{3/2}$, as shown in Fig. 5 as the green stars.

05 Beam Dynamics and Electromagnetic Fields

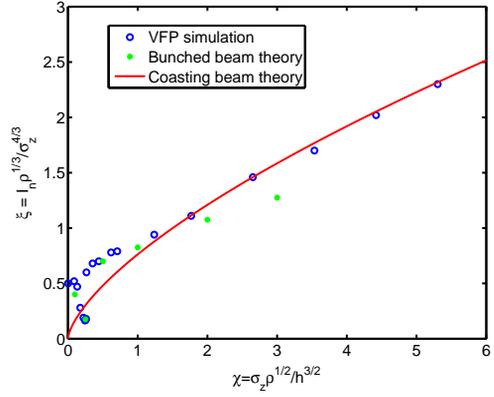**D03 High Intensity in Circular Machines**

Figure 5: Threshold ξ^{th} as a function of the shielding parameter χ. The circles are the result of the VFP simulation[7].

The solid line in the figure is plotted using the formula, $\xi = 3\sqrt{2}\chi^{2/3}/\pi^{3/2}$. It can be derived from the coasting beam threshold in Eq. (12) using the definitions of ξ and χ and Eq. (19). Clearly, the agreement between the simulation and the coasting beam theory is excellent when $\chi > 2$. Finally, the bunched beam theory confirms the dip at $\chi = 0.25$, seen first in the simulation.

Finally, for the theoretical ξ^{th}, one may simplify the result in the figure to

$$\xi^{th}(\chi) = 0.5 + 0.34\chi, \tag{27}$$

except the dip at $\chi = 0.25$. This linear relation was first obtained by fitting to the result of the VFP simulation[7].

COMPARISON TO THE MEASUREMENTS

Although the bursting phenomenon at THz was observed under various momentum compaction factors, RF voltages, bunch lengths, and energies in many synchrotron light sources, its threshold current I_b^{th} satisfies a simple scaling law[13] with respect to the bunch length σ_z (in MKS units),

$$\sigma_z^{7/3} = \frac{c^2 Z_0}{2\pi F 3^{1/3}} I_b^{th} \rho^{1/3}/(V_{rf} f_{rf} f_{rev}), \tag{28}$$

where F is a constant. Note that σ_z is the bunch length at zero current not at the threshold current. This scaling property with $F = 7.456$ was derived[14] based on the coasting beam theory developed by Stupakov and Heifets[1]. It agrees very well with the BESSY II measurement[15].

A similar equation can be derived easily from the bunched beam theory. Starting from $\xi = I_n \rho^{1/3}/\sigma_z^{4/3}$ and using Eqs. (19), (14), and (13), we obtain (in MKS units)

$$\sigma_z^{7/3} = \frac{c^2 Z_0}{8\pi^2 \xi} I_b \rho^{1/3}/(V_{rf}\cos\phi_s f_{rf} f_{rev}). \tag{29}$$

Here we have used $Z_0 = 4\pi/c$ to change from CGS units to MKS units. So far, this is merely a general relation between

the scaled current ξ and the bunch current I_b. In particular, applying it to the threshold, we have (in MKS units)

$$\sigma_z^{7/3} = \frac{c^2 Z_0}{8\pi^2 \xi^{th}(\chi)} I_b^{th} \rho^{1/3} / (V_{rf} \cos\phi_s f_{rf} f_{rev}), \quad (30)$$

where $\xi^{th}(\chi)$ is given by Eq. (27), ignoring the dip.

For very short bunches, the shielding parameter is so small that one can use $\xi^{th} = 0.5$ in Eq. (30) to make a comparison with the threshold measurement. Such a measurement[16] was carried out at different momentum compaction factors with the same RF voltage at ANKA. The result is shown in Fig. 6. As one can see, the agreement between the theory and the measurement is excellent.
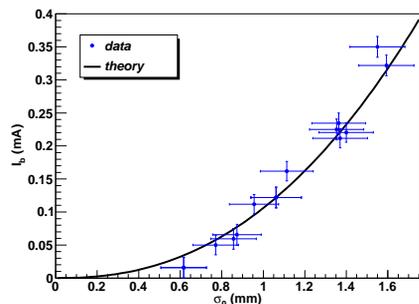

Figure 6: (courtesy of M. Klein) Measured bursting threshold as as function of σ_z at ANKA. $\xi^{th} = 0.5$ in Eq. (30) is used for the solid curve.

In most storage rings, $\cos\phi_s$ is nearly equal to 1. As a result, Eqs. (28) and (30) are almost identical provided

$$F = 4\pi \xi^{th}(\chi)/3^{1/3}. \quad (31)$$

In contrast to the coasting beam theory, F is not a constant but rather a function of the shielding parameter χ. Indeed, there is some experimental evidence shown in Table 2 to support this claim.

Table 2: Comparison of Theory with Measurements at Various Synchrotron Light Sources

Machine	F (meas.)	F (theory)	χ
BESSY II	7.46	5.84	0.48
MLS	3.40	5.23	0.29
ANKA	4.36	5.58	0.42
Diamond	2.90	1.48	0.25

In the table, the measured values of F were provided by Wustefeld for BESSY II and MLS, Klein for ANKA, and Martin for Diamond. The theoretical values are calculated using Eqs. (31) and (27), except for the Diamond Light Source, for which $\xi = 0.17$ is used for the dip. Moreover, the measurements at Diamond were carried out with the negative momentum compaction factors. Therefore, for that one, its threshold has to be recalculated. As one can

see, the agreement is not perfect but reasonably good considering that only the CSR impedance is included in the theory.

CONCLUSION

For a long bunch, $\chi = \sigma_z \rho^{1/2} / h^{3/2} > 2$, the coasting beam theory with the shielding impedance works well. Eq. (12) should be used for estimating the threshold.

When a bunch is short, $\chi < 2$, the bunched beam theory should be applied. According to Eq. (30), the beam becomes unstable if

$$I_b > \frac{8\pi^2 \xi^{th}(\chi) \sigma_z^{7/3} V_{rf} \cos\phi_s f_{rf} f_{rev}}{c^2 Z_0 \rho^{1/3}}. \quad (32)$$

A shorter bunch is always more unstable. However, it is much better to reduce the bunch length with an increase in RF voltage than with a decrease of the momentum compaction factor.

ACKNOWLEDGEMENT

REFERENCES

[1] G. Stupakov and S. Heifets, Phys. Rev. ST Accel. Beams **5**, 054402 (2002).

[2] J.B. Murphy, S. Krinsky, and R.L. Gluckstern, Part. Accel. **57**, 9 (1997).

[3] A. Faltens and L.J. Laslett, Part. Accel. **4**, 151 (1973).

[4] J. Byrd *et al.* , Phys. Rev. Lett. **89**, 224801 (2002).

[5] R.L. Warnock, SLAC-PUB-5379 November (1990).

[6] F.W.J. Olver, *Asymptotics and Special Functions,* Academic Press, New York, (1974).

[7] K.L.F. Bane, Y. Cai, and G. Stupakov, Phys. Rev. ST Accel. Beams **13**, 104402 (2010).

[8] G.L. Carr *et at.*, Nucl. Instrum. Methods Phys. Res. Sect. A **463**, 387 (2001).

[9] M. Sands, SLAC Report No. 121, (1979).

[10] J. Haissinski, Nuovo Cimenta B **18**, 72 (1973).

[11] K. Oide and K. Yokoya, KEK Report No. 90-10, (1990).

[12] Y. Cai, Phys. Rev. ST. Accel. Beams **14**, 061002 (2011).

[13] G. Wustefeld *et al.*, Proceedsings of IPAC'10, Kyoto, Japan, p. 2508 (2010).

[14] F. Sannibale *et al.*, Phys. Rev. Lett. **93**, 094801 (2004).

[15] J. Feikes *et al.*, Proceedings of EPAC 2004, Lucerne, Switzerland, p. 1954 (2004).

[16] M. Klein *et al.*, Proceedings of PAC09, Vancouver, BC, Canada, p. 4761 (2009).

05 Beam Dynamics and Electromagnetic Fields

D03 High Intensity in Circular Machines